UF College of Public Health and Health Professions
Department of Environmental and Global Health
UNIVERSITY of FLORIDA

Integrating machine learning and quantitative structure activity relationship modeling approaches to build an artificial intelligence-assisted physiologically based pharmacokinetic model for nanoparticles in tumor-bearing mice

---- Society for Risk Analysis
---- Dose Response Specialty Group in September 2023

Wei-Chun Chou

Center for Environmental and Human Toxicology (CEHT)
Department of Environmental and Global Health, College of Public Health and Health Professions
University of Florida, Gainesville, FL 32610

Challenge in tumor delivery of nanomedicine

- NPs are becoming an increasingly popular tool for biomedical imaging and drug delivery.

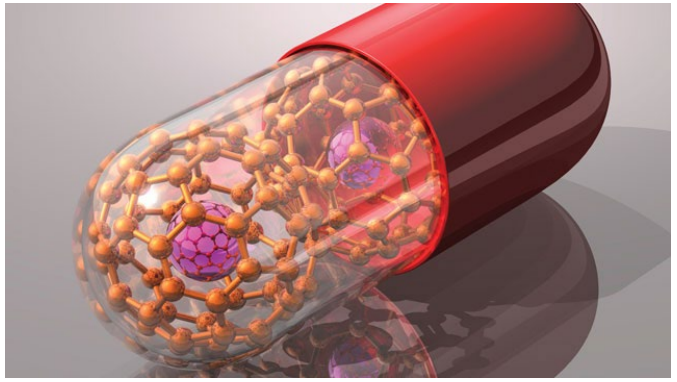

Image source: https://www.the-scientist.com/cover-story/nanomedicine-37087

- The poor tumor delivery efficiency of nanomedicines has been a major barrier in the translation of nanomedicine to potent drug candidates.
- Lack of understanding of pharmacokinetic of nanomedicine might be a major reason.

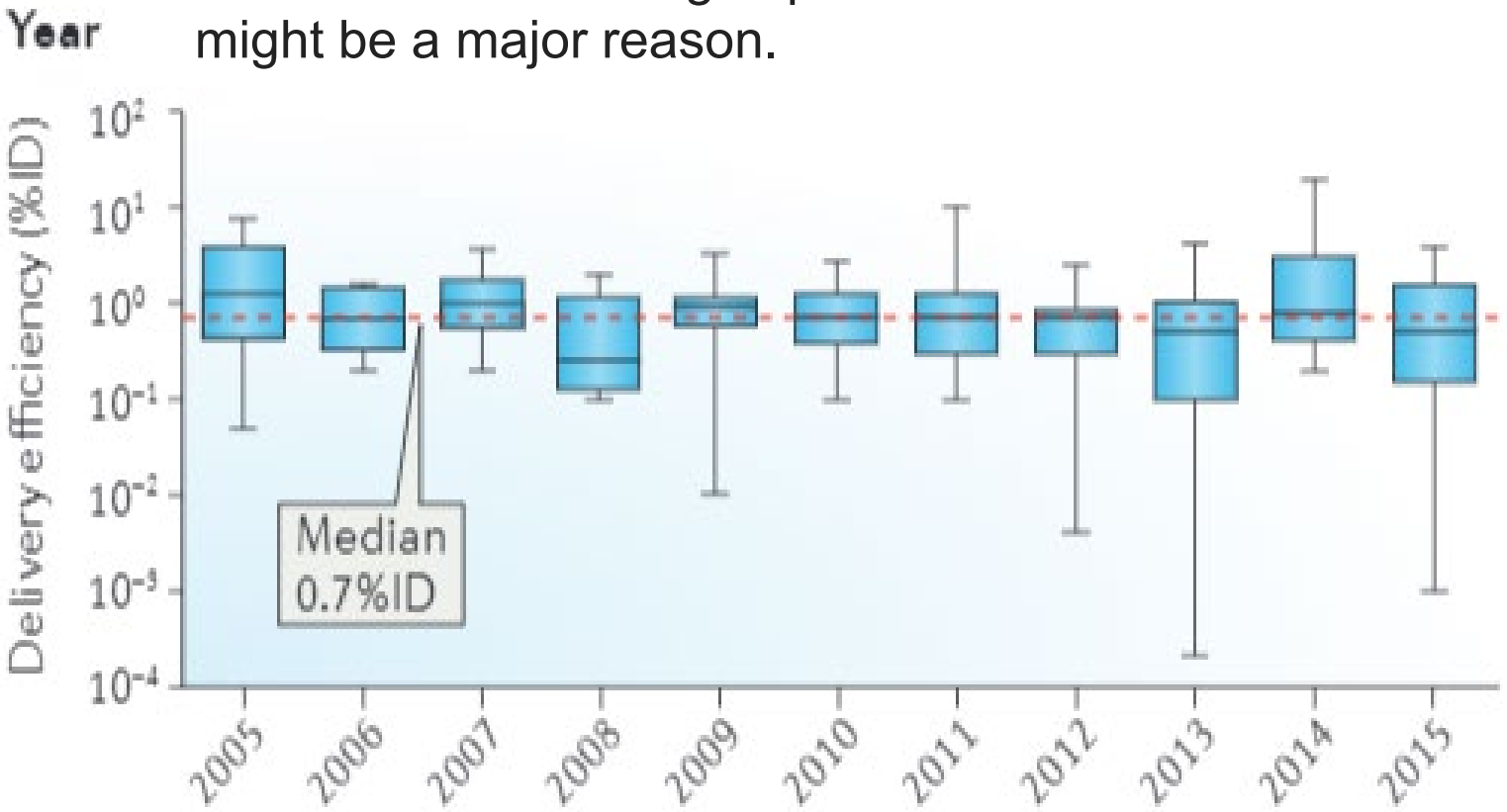

Image was obtained from Wilhelm et al., 2016

Abbreviations: Nanoparticles (NPs)

Biodistribution of Nanoparticles (NPs)

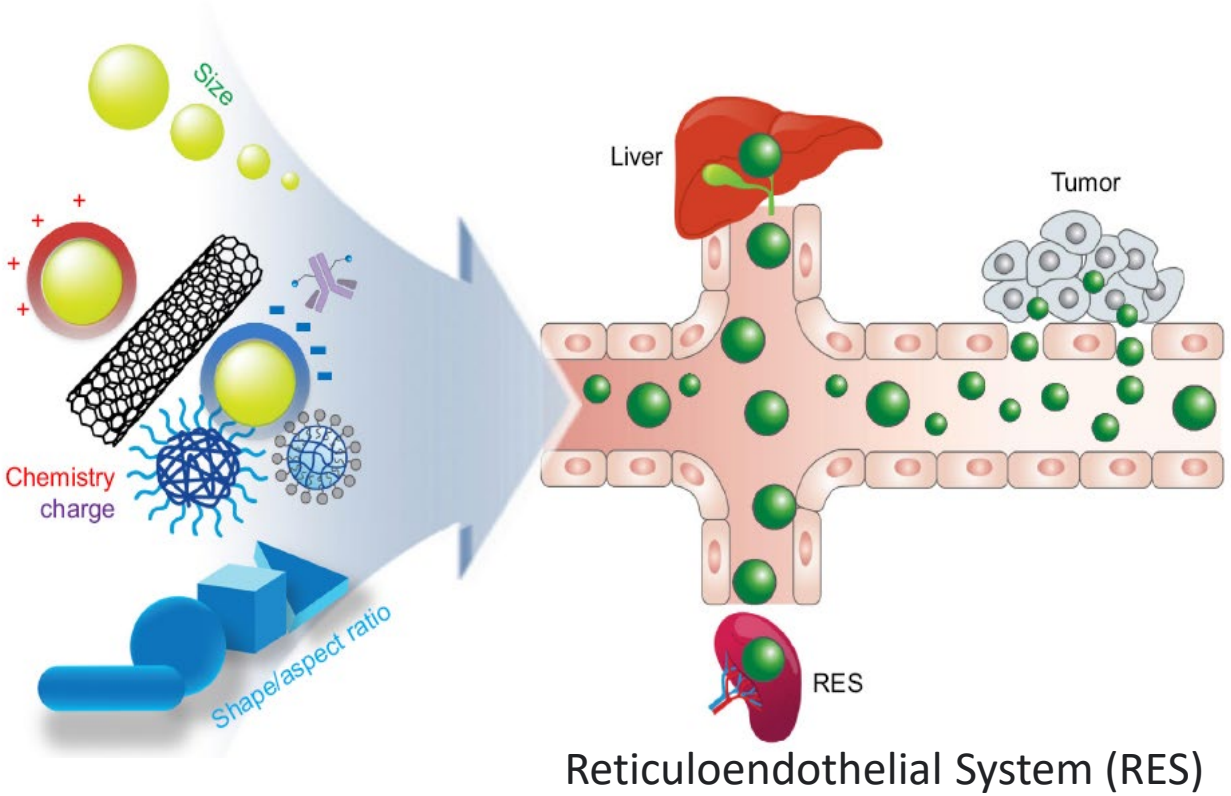

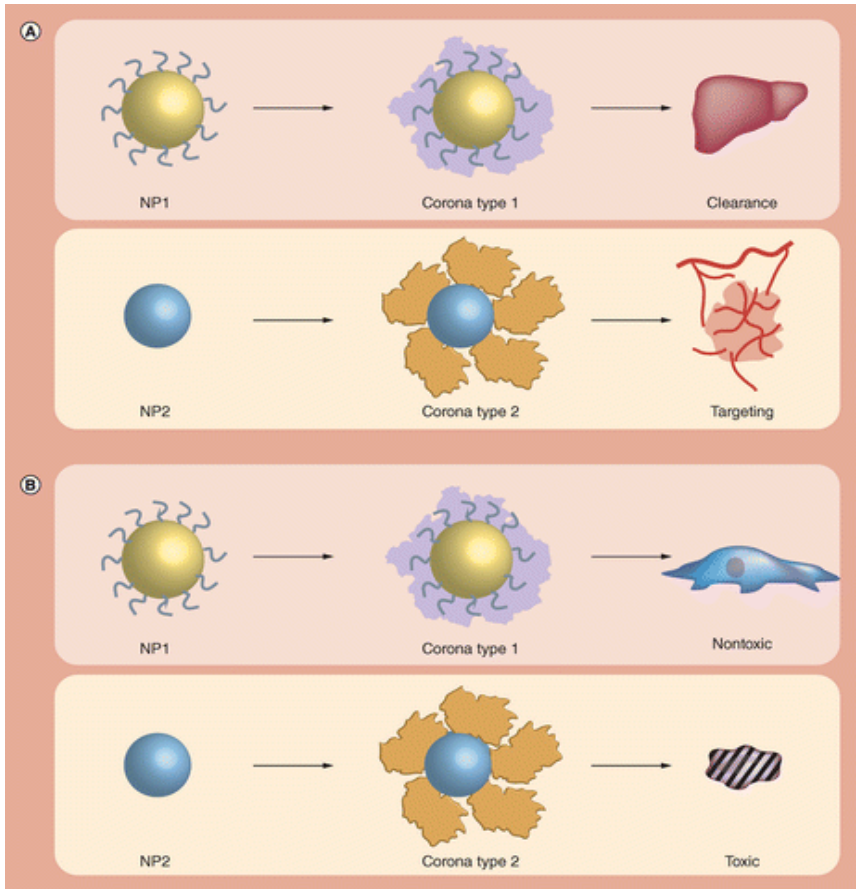

- The pharmacokinetics of nanomedicine is very different with the traditional drugs.
- One of important mechanisms to affect the NPs' biodistribution is **phagocytosis.**
- Different physicochemical properties of NPs, such as size, materials, biochemistry, and shape, may relate to the NPs' phagocytosis and biodistribution.

Kim et al., 2015; Hamad-Schifferli et al., 2015

Two AI methods were applied to predict tumor delivery efficiency

1. A data-driven method

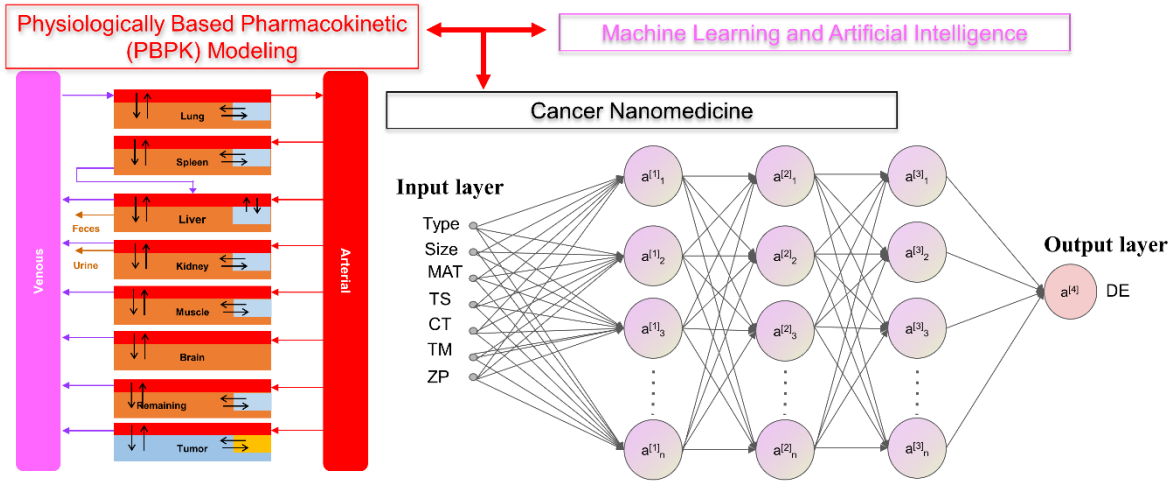

Lin Z, Chou WC, Cheng YH, He C, Monteiro-Riviere NA, Riviere JE. Predicting Nanoparticle Delivery to Tumors Using Machine Learning and Artificial Intelligence Approaches. Int J Nanomedicine. 2022 Mar 24;17:1365-1379. doi: 10.2147/IJN.S344208.

2. A hybrid method

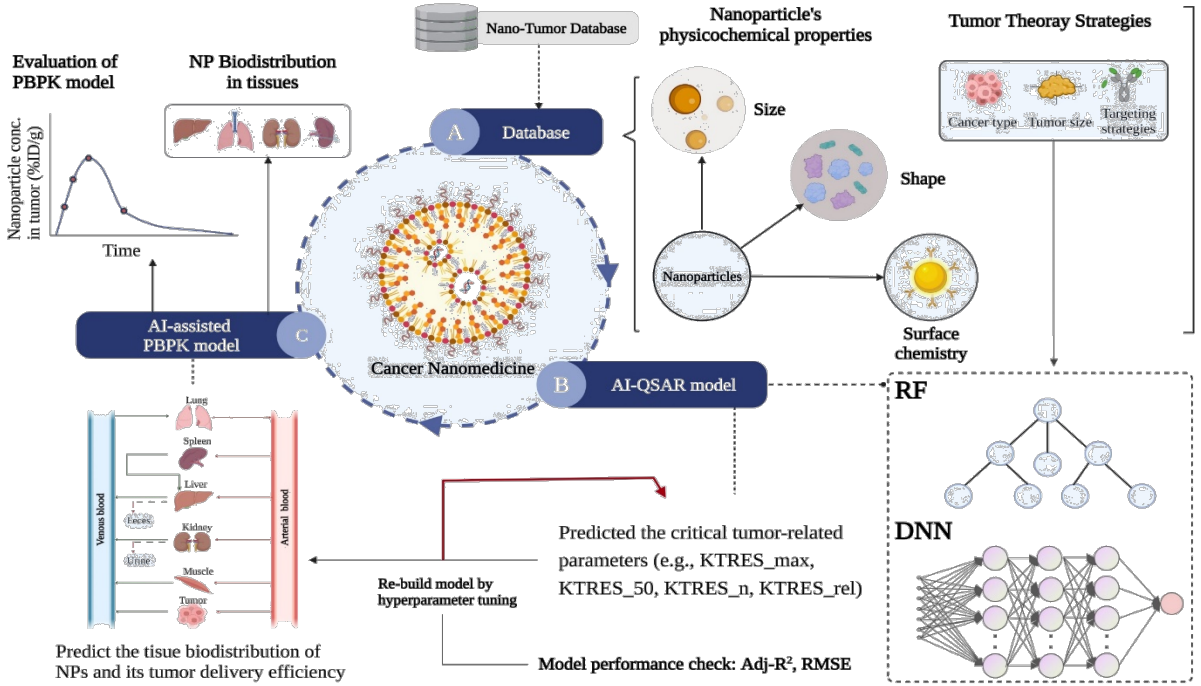

Chou WC, Chen Q, Yuan L, Cheng YH, He C, Monteiro-Riviere NA, Riviere JE, Lin Z. An artificial intelligence-assisted physiologically-based pharmacokinetic model to predict nanoparticle delivery to tumors in mice. J Control Release. 2023 Sep;361:53-63. doi: 10.1016/j.jconrel.2023.07.040.

A data-driven model (with QSAR approach)

Physiologically Based Pharmacokinetic (PBPK) Modeling

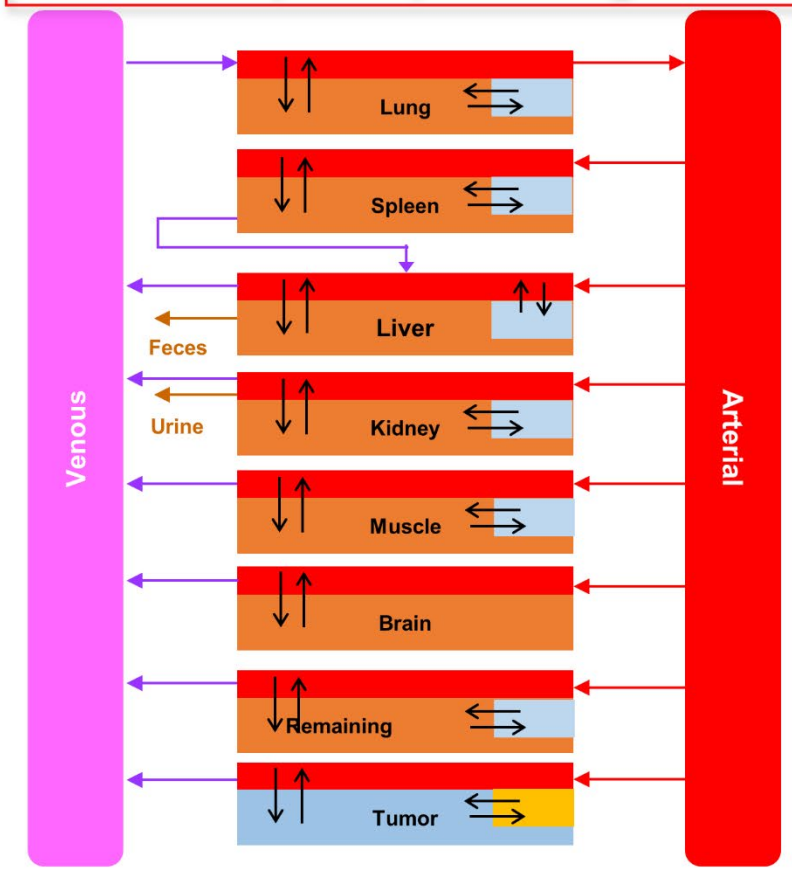

Machine Learning and Artificial Intelligence

Cancer Nanomedicine

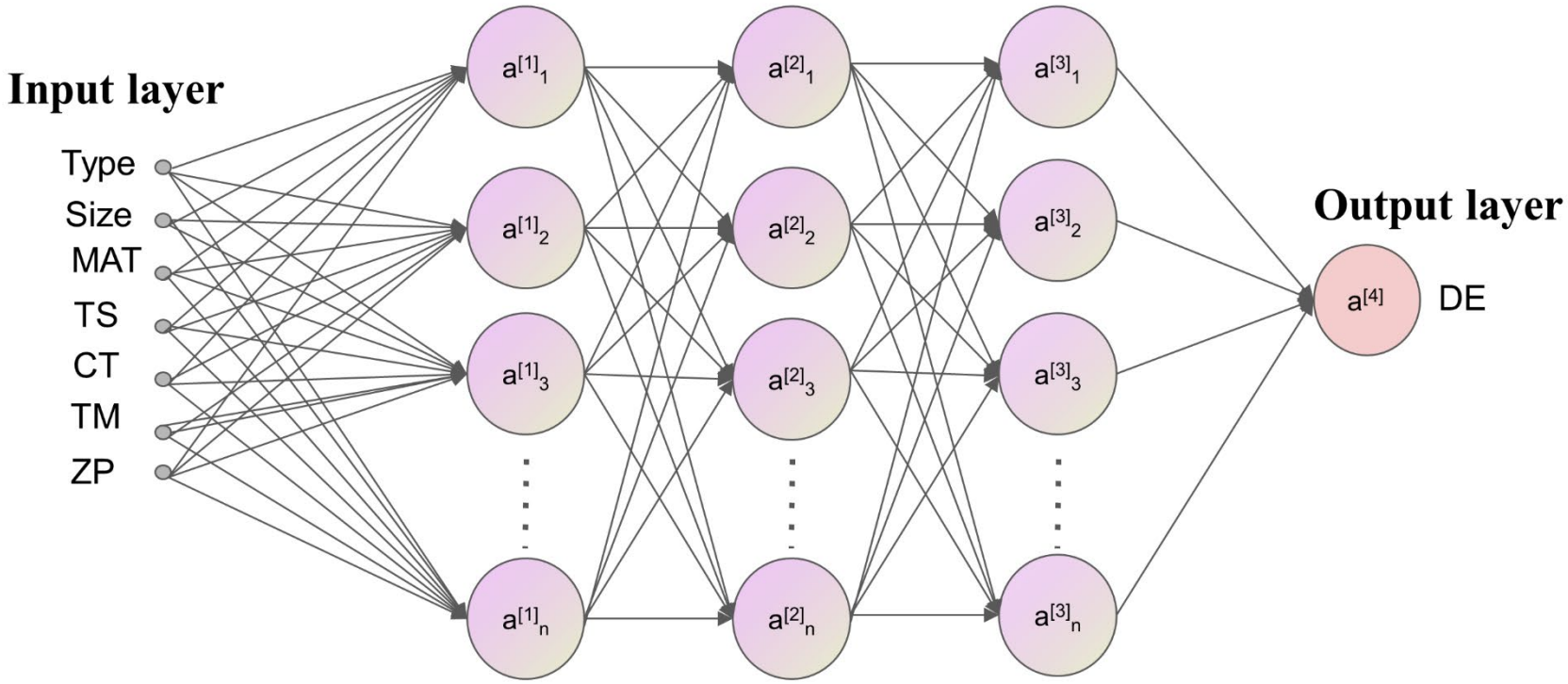

Quantitative structure-activity relationship (QSAR)

Lin Z*, Chou WC, Cheng YH, He C, Monteiro-Riviere NA, Riviere JE. (2022). Predicting Nanoparticle Delivery to Tumors Using Machine Learning and Artificial Intelligence Approaches. *International Journal of Nanomedicine*, 17: 1365-1379.

Variables in the Nano-Tumor Database

1. Categorical variables

- Material: Inorganic/organic NPs →1/0
- Shape: Spherical/Rod/circle → 1…3
- Cancer type: Brain/Breast/…
- Tumor model (TM)
- Targeting strategy (TS): Active/Passive →1/0

2. Numerical variables

- Hydrodynamic diameter [nm]
- Zeta potential [mV]

3. Target variables

- Tumor Delivery efficiency (%ID)

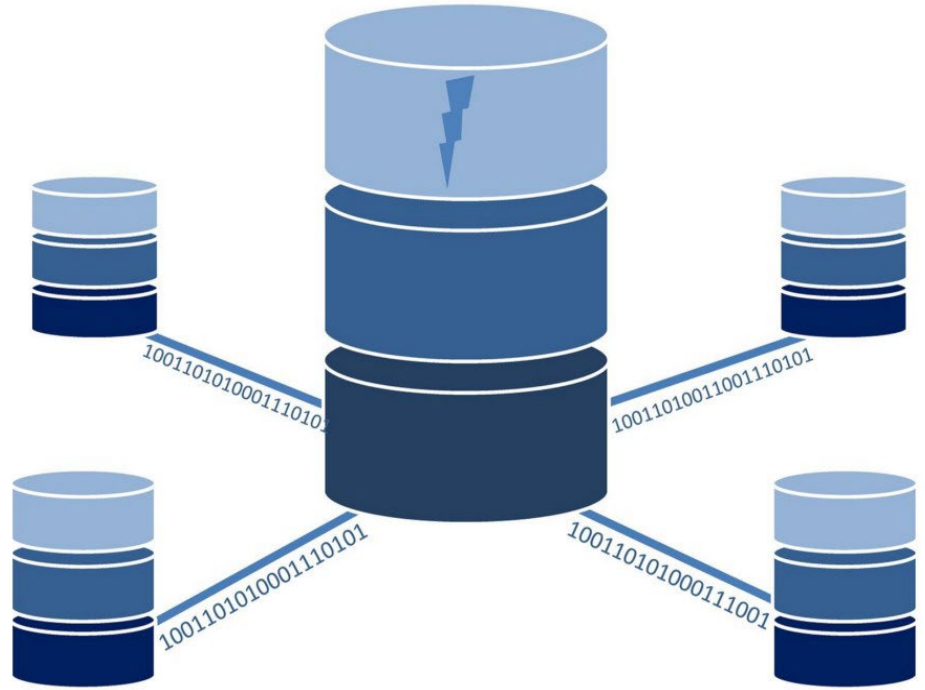

Image by Tumisu from Pixabay

Overview of the Nano-Tumor Database (1/3): Categorical variables

NPs type

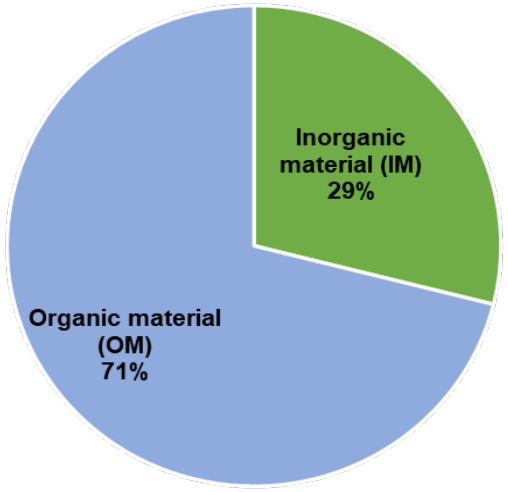

NPs shape

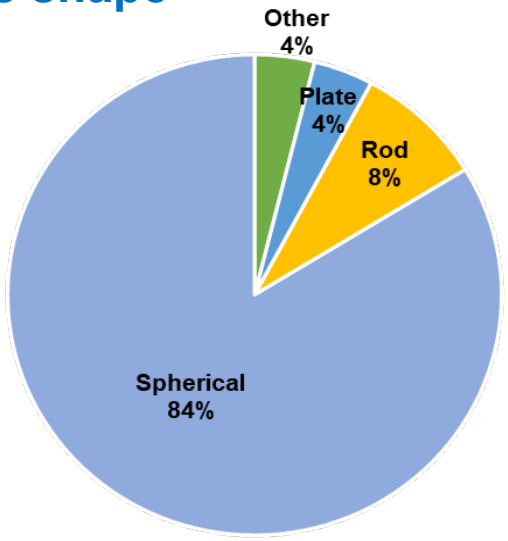

Materials

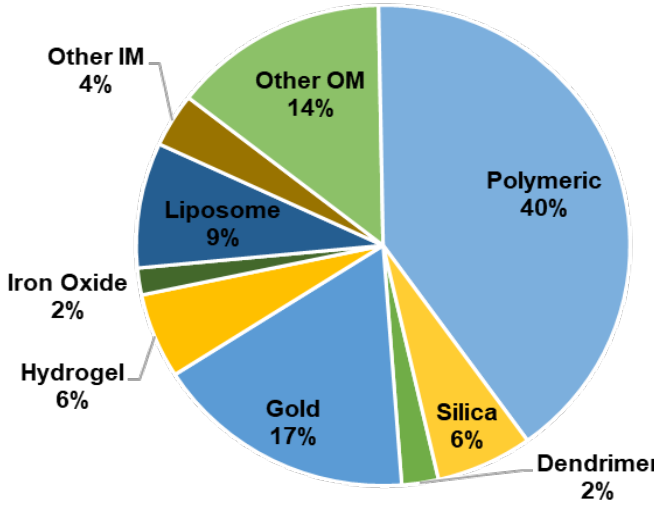

Targeting Strategy (TS)

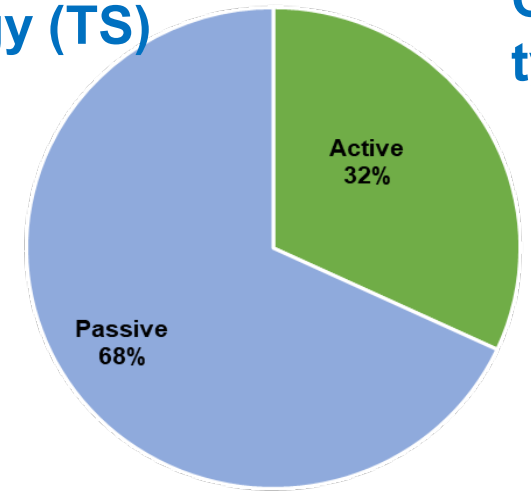

Cancer type (CT)

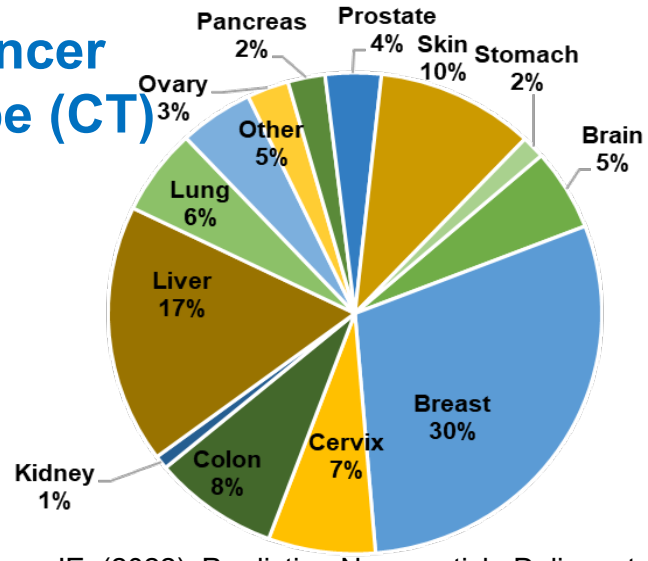

Tumor model (TM)

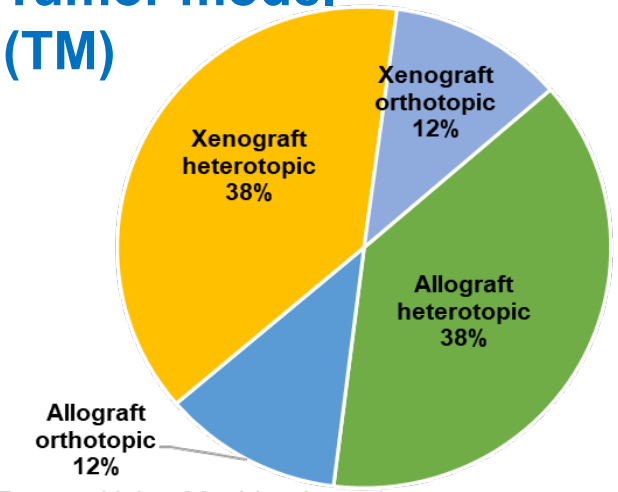

Lin Z*, Chou WC, Cheng YH, He C, Monteiro-Riviere NA, Riviere JE. (2022). Predicting Nanoparticle Delivery to Tumors Using Machine Learning and Artificial Intelligence Approaches. *International Journal of Nanomedicine*, 17: 1365-1379.

Overview of the Nano-Tumor Database (2/3): Numerical variables

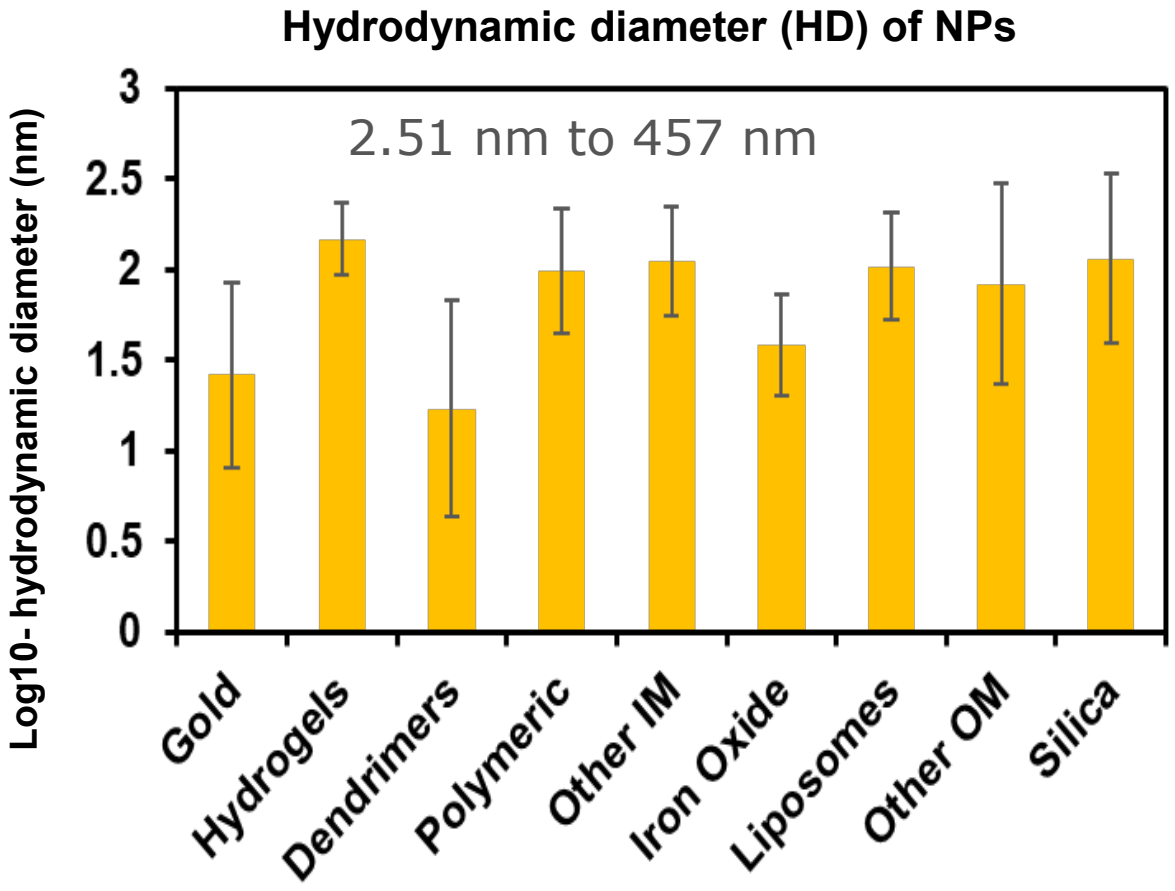

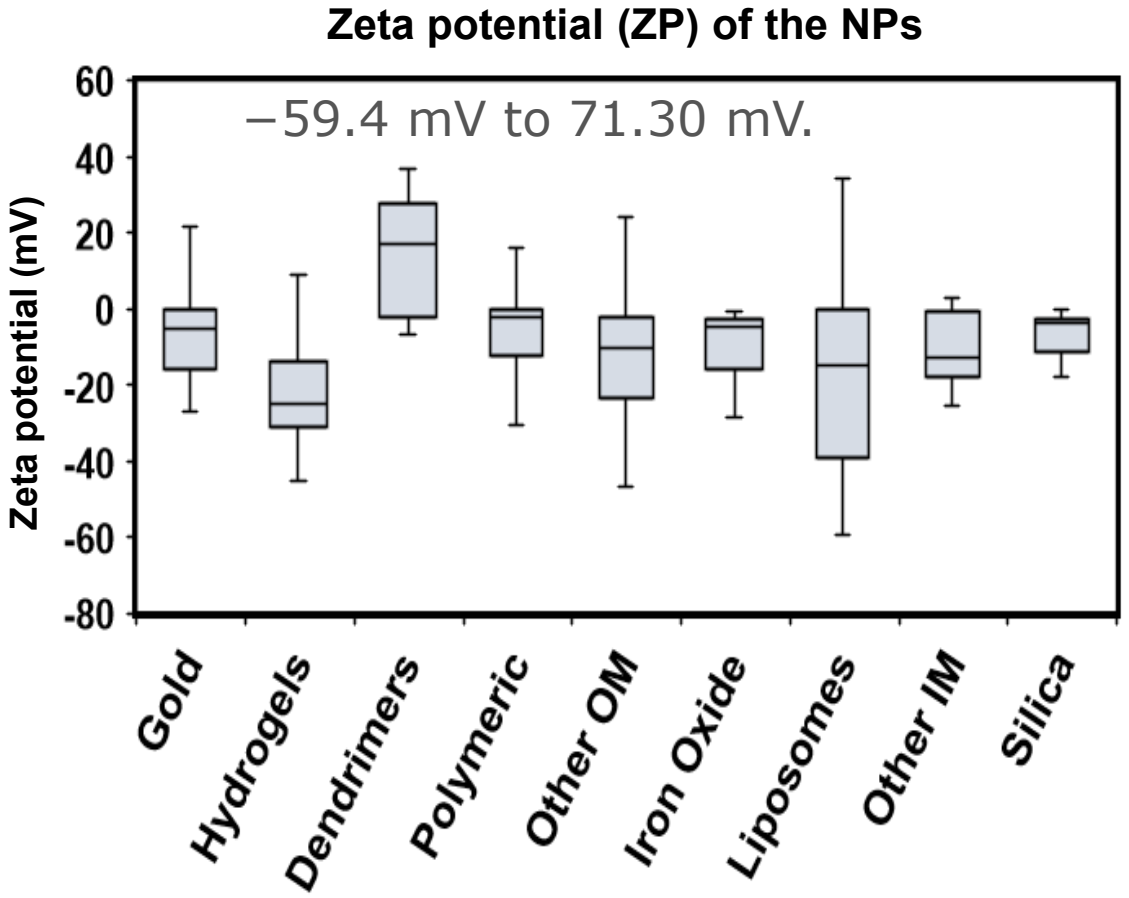

Lin Z*, Chou WC, Cheng YH, He C, Monteiro-Riviere NA, Riviere JE. (2022). Predicting Nanoparticle Delivery to Tumors Using Machine Learning and Artificial Intelligence Approaches. *International Journal of Nanomedicine*, 17: 1365-1379.

Overview of the Nano-Tumor Database (3/3): Target variables

Estimation of tumor delivery efficiency (DE)

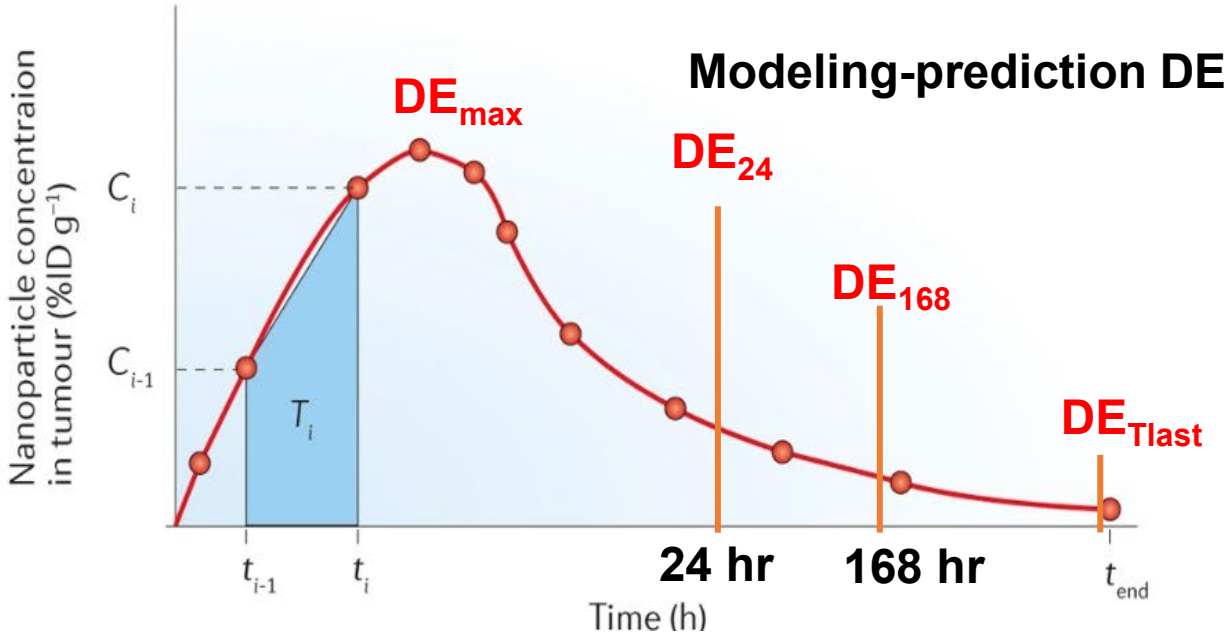

$$\text{Trapezoid } (T_i) = 0.5\,(C_i + C_{i-1})\,(t_i - t_{i-1}) \quad (1)$$

$$\text{AUC}_{\text{Tumour}} = \sum_{i=1}^{n} T_i \quad (2)$$

$$\text{Delivery efficiency} = \frac{\text{AUC}_{\text{Tumour}}}{t_{\text{end}}}\,(m_{\text{Tumour}}) \quad (3)$$

- The linear trapezoidal method is limited to the dataset and can not estimate the DE at different time points such as 24 (DE24), 168 (DE168) and last time point (DETlast)
- In this study, we used calibrated PBPK model to estimate the AUC and then estimate the Demax, DE24, DE168 and DETlast

Wilhelm et al. (2016)

Machine Learning and Artificial Intelligence models

Table 1. Summary of modeling algorithms used in this study.

Model	Synonym	Model category	Tuning parameters
Machine Learning Algorithms			
Linear regression	Linear	Simple model	Alpha, Lambda
k-nearest neighbors	Knn	Simple model	K
Random Forest	RF	Ensemble model	mtry
Bagged Model	Bag	Ensemble model	None[a]
Stochastic Gradient Boosting	Gbm	Ensemble model	n.trees; shrinkage, n.minobsinnode
Support vector machine	SVM	Support vector machine	C
Least-squares SVM	LS-SVM	Support vector machine	Cost, loss
L2-Regularized SVM	L2-SVM	Support vector machine	Cost, loss
Deep Learning Algorithm			
Deep neural networks	DNN	Neural networks	Rate, L1, L2

Lin Z*, Chou WC, Cheng YH, He C, Monteiro-Riviere NA, Riviere JE. (2022). Predicting Nanoparticle Delivery to Tumors Using Machine Learning and Artificial Intelligence Approaches. *International Journal of Nanomedicine*, 17: 1365-1379.

Evaluation metrics for machine learning models

The performance of each model for the 5-fold cross-validation and external validation was evaluated by root mean square error (RMSE), mean absolute error (MAE) and adjusted determination coefficient (R^2).

$$RMSE = \sqrt{\frac{1}{n} \cdot \left(\sum (y - \hat{y})^2\right)} \quad (1)$$

$$MAE = \frac{1}{n} \cdot \left(\sum |y - \hat{y}|\right) \quad (2)$$

$$R^2 = 1 - \left(\sum (y - \hat{y})^2 / \sum (y - \bar{y})^2\right) \quad (3)$$

Comparison of predictions between linear regression, machine learning and deep learning models

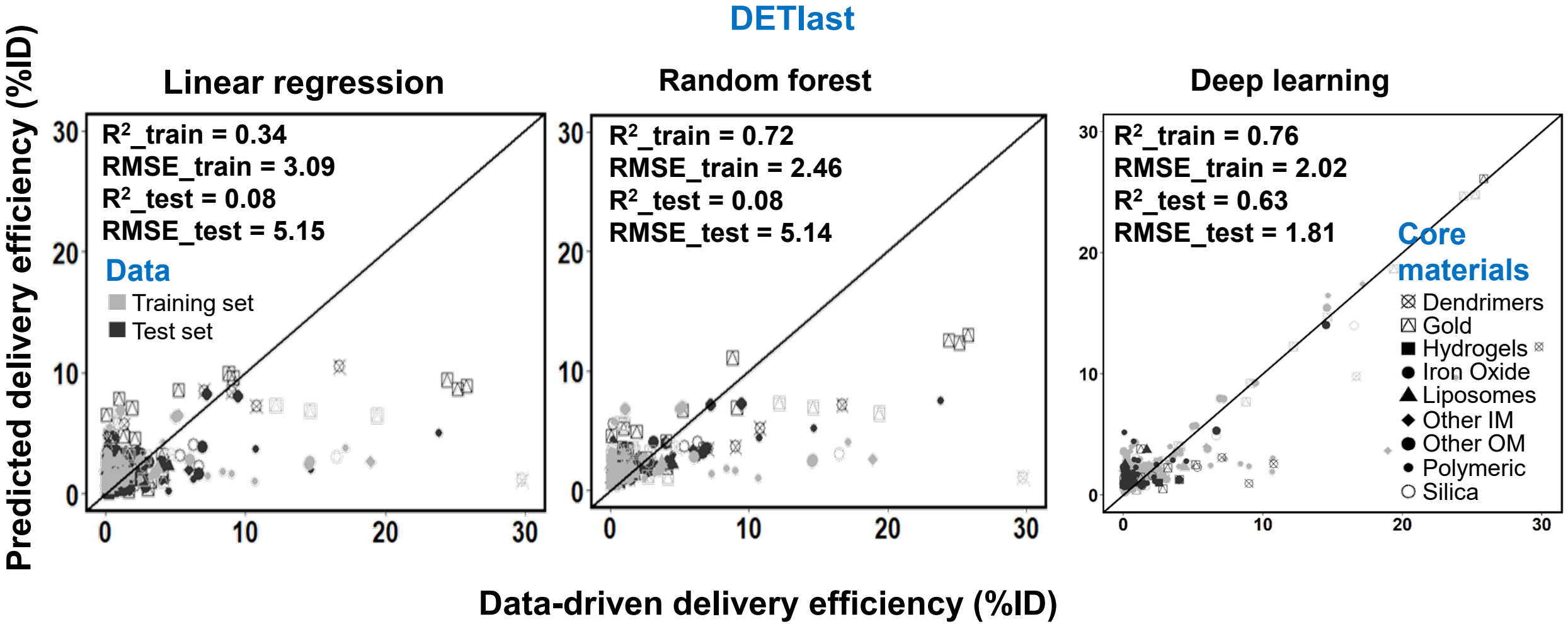

Lin Z*, Chou WC, Cheng YH, He C, Monteiro-Riviere NA, Riviere JE. (2022). Predicting Nanoparticle Delivery to Tumors Using Machine Learning and Artificial Intelligence Approaches. *International Journal of Nanomedicine*, 17: 1365-1379.

5-fold cross validation results using machine learning and deep learning

	DE_{max}		DE_{24}		DE_{168}		DE_{Tlast}	
Model	5-fold CV	Test	5-fold CV	Test	5-fold CV	Test	5-fold CV	Test
LR								
R^2	0.06 ± 0.05	0.08	0.10 ± 0.10	0.08	0.07 ± 0.03	0.06	0.07 ± 0.07	0.13
RMSE	3.98 ± 1.03	7.56	3.89 ± 0.61	6.56	2.18 ± 0.60	3.20	3.98 ± 0.88	4.73
MAE	2.42 ± 0.48	3.31	2.37 ± 0.24	2.70	1.29 ± 0.20	1.44	2.42 ± 0.44	2.46
KNN								
R^2	0.03 ± 0.04	0.06	0.04 ± 0.04	0.08	0.03 ± 0.04	0.04	0.01 ± 0.04	0.08
RMSE	4.05 ± 1.12	7.55	3.95 ± 0.71	6.51	2.31 ± 0.56	3.22	4.05 ± 1.01	4.77
MAE	2.36 ± 0.47	3.51	2.31 ± 0.30	2.82	1.33 ± 0.21	1.50	2.36 ± 0.43	2.59
RF								
R^2	0.19 ± 0.12	0.16	0.19 ± 0.16	0.17	0.19 ± 0.10	0.11	0.15 ± 0.16	0.29
RMSE	3.71 ± 1.03	7.15	3.64 ± 0.62	6.18	2.06 ± 0.61	3.17	3.72 ± 0.82	4.24
MAE	2.21 ± 0.48	2.92	2.17 ± 0.27	2.37	1.20 ± 0.21	1.30	2.22 ± 0.45	2.15
Bag								
R^2	0.09 ± 0.07	0.08	0.13 ± 0.12	0.08	0.10 ± 0.06	0.04	0.09 ± 0.09	0.15
RMSE	3.91 ± 1.06	7.49	3.86 ± 0.64	6.50	2.16 ± 0.58	3.22	3.91 ± 0.91	4.63
MAE	2.38 ± 0.47	3.34	2.34 ± 0.25	2.66	1.27 ± 0.19	1.35	2.38 ± 0.46	2.44
Gbm								
R^2	0.08 ± 0.08	0.09	0.12 ± 0.11	0.17	0.11 ± 0.06	0.05	0.08 ± 0.07	0.24
RMSE	3.91 ± 1.03	7.48	3.81 ± 0.62	6.30	2.16 ± 0.57	3.22	3.92 ± 0.85	4.46
MAE	2.42 ± 0.47	3.27	2.34 ± 0.26	2.60	1.30 ± 0.20	1.32	2.42 ± 0.42	2.38
R-SVM								
R^2	0.02 ± 0.03	0.23	0.04 ± 0.03	0.19	0.04 ± 0.03	0.14	0.02 ± 0.02	0.25
RMSE	4.12 ± 1.29	7.80	4.02 ± 0.87	6.76	2.28 ± 0.67	3.31	4.12 ± 1.12	4.97
MAE	1.93 ± 0.54	2.82	1.87 ± 0.35	2.32	1.06 ± 0.24	1.22	1.93 ± 0.47	2.08
LS-SVM								
R^2	0.02 ± 0.03	0.23	0.05 ± 0.03	0.18	0.05 ± 0.03	0.13	0.03 ± 0.03	0.24
RMSE	4.12 ± 1.29	7.81	4.02 ± 0.87	6.77	2.27 ± 0.66	3.31	4.12 ± 1.12	4.98
MAE	1.92 ± 0.54	2.83	1.86 ± 0.26	2.32	1.05 ± 0.24	1.22	1.93 ± 0.47	2.09
L2-SVM								
R^2	0.07 ± 0.06	0.14	0.11 ± 0.10	0.14	0.08 ± 0.04	0.18	0.08 ± 0.07	0.19
RMSE	4.01 ± 0.97	7.32	3.91 ± 0.59	6.37	2.23 ± 0.56	3.03	4.02 ± 0.78	4.54
MAE	2.52 ± 0.46	3.20	2.45 ± 0.26	2.61	1.38 ± 0.19	1.37	2.52 ± 0.42	2.39
DNN								
R^2	0.47 ± 0.20	0.70	0.40 ± 0.34	0.46	0.45 ± 0.24	0.33	0.35 ± 0.23	0.63
RMSE	3.58 ± 1.35	2.38	2.75 ± 0.92	3.10	1.96 ± 1.09	1.78	3.24 ± 1.04	3.01
MAE	2.20 ± 0.65	1.64	1.72 ± 0.50	1.84	1.10 ± 0.42	0.94	1.92 ± 0.54	1.81

Table Footnote

LR: Linear regression, KNN: k-nearest neighbors; RF: Random forest; Bag: Bagged Model; Gbm: Stochastic Gradient Boosting; R-SVM: Regular support vector machine; LS-SVM: least-squared support vector machine; L2-SVM: L2-regulated support vector machine; DNN: Deep learning neural network. DE_{max}, DE_{24}, DE_{168} and DE_{Tlast} represent the maximum tumor delivery efficiency (DE), DE at 24 h, 168 h, and the last sampling time, respectively. CV: cross-validation.

Lin Z*, Chou WC, Cheng YH, He C, Monteiro-Riviere NA, Riviere JE. (2022). Predicting Nanoparticle Delivery to Tumors Using Machine Learning and Artificial Intelligence Approaches. *International Journal of Nanomedicine*, 17: 1365-1379.

Importance percentage in the deep learning model for each target variable

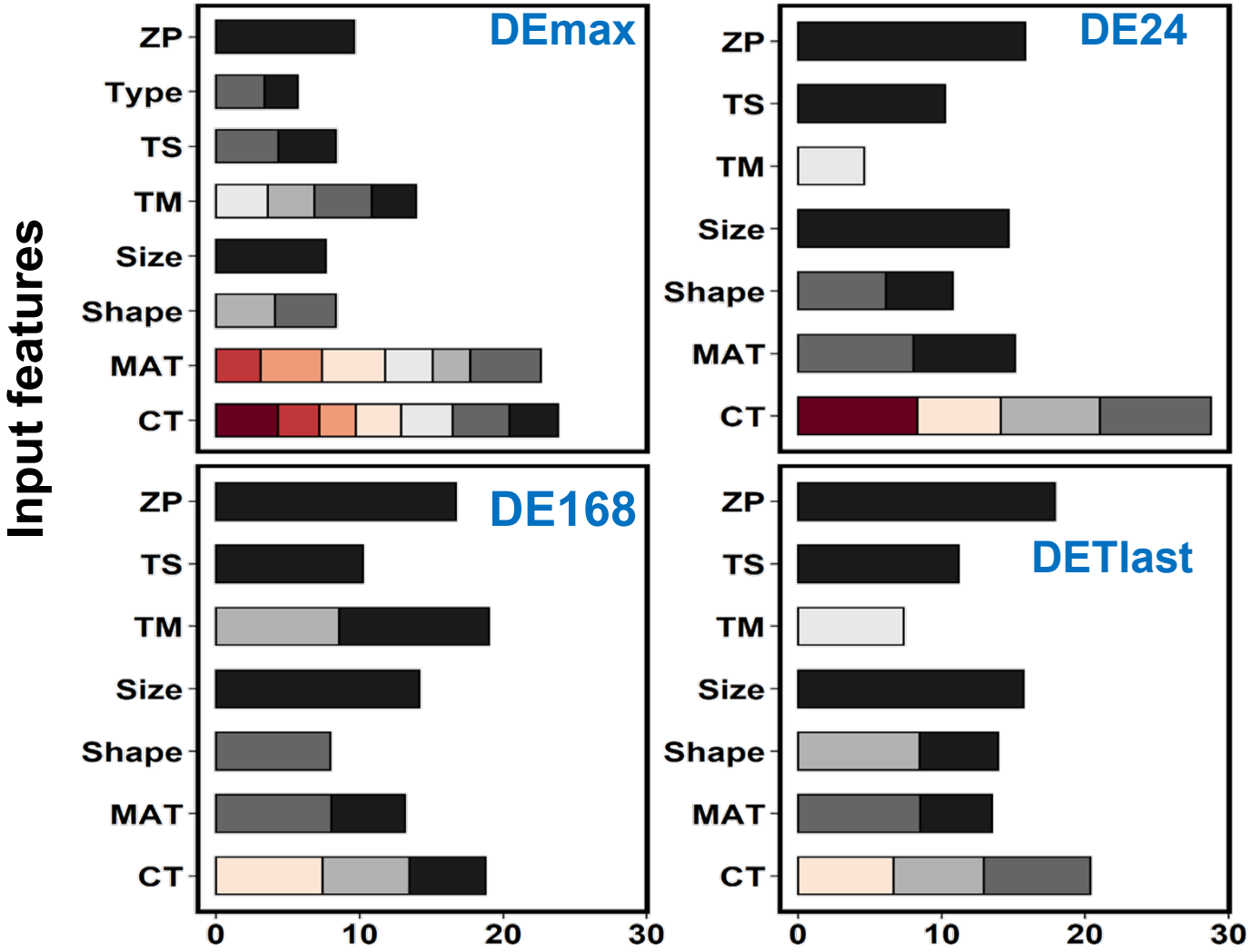

DE24: Delivery efficiency at 24 hours
DE168: Delivery efficiency at 168 hours
Demax: Maximal delivery efficiency
Delast: Delivery efficiency at last time point

Lin Z*, Chou WC, Cheng YH, He C, Monteiro-Riviere NA, Riviere JE. (2022). Predicting Nanoparticle Delivery to Tumors Using Machine Learning and Artificial Intelligence Approaches. *International Journal of Nanomedicine*, 17: 1365-1379.

Summary for data-driven method

- Deep learning model had the best predictive performance compared to all other methods.
- Zeta potential and NPs materials were the most important factors which contribute to the tumor delivery efficiency.
- The present study also demonstrates the feasibility of integrating ML/AI with PBPK models to support cancer nanomedicine research and development.

Lin Z*, Chou WC, Cheng YH, He C, Monteiro-Riviere NA, Riviere JE. (2022). Predicting Nanoparticle Delivery to Tumors Using Machine Learning and Artificial Intelligence Approaches. *International Journal of Nanomedicine*, 17: 1365-1379.

A hybrid method (AI-assisted PBPK model)

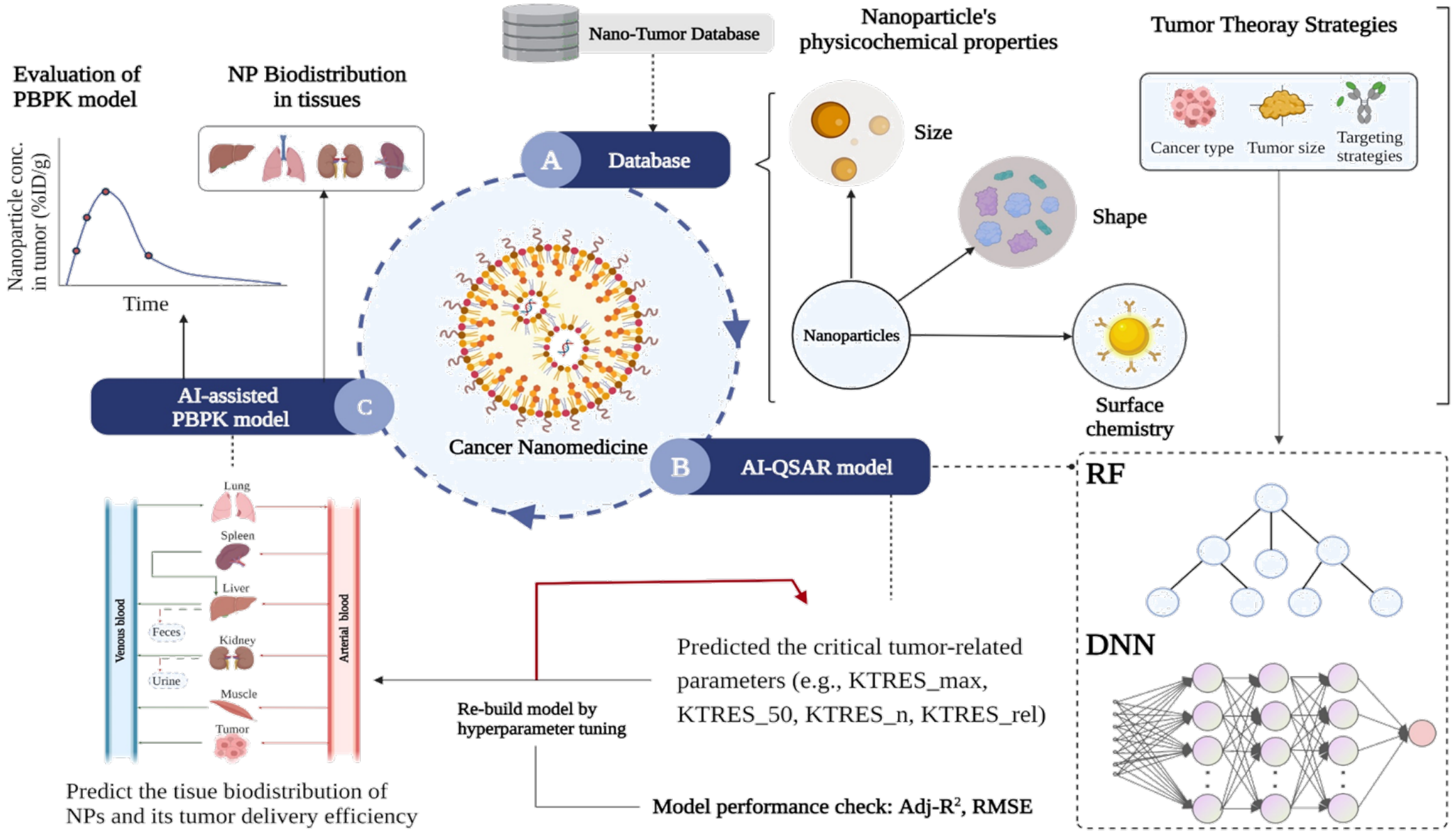

Chou WC, Chen Q, Yuan L, Cheng YH, He C, Monteiro-Riviere NA, Riviere JE, Lin Z. An artificial intelligence-assisted physiologically-based pharmacokinetic model to predict nanoparticle delivery to tumors in mice. J Control Release. 2023 Sep;361:53-63

Theoretical parameter: Endocytosis of NPs

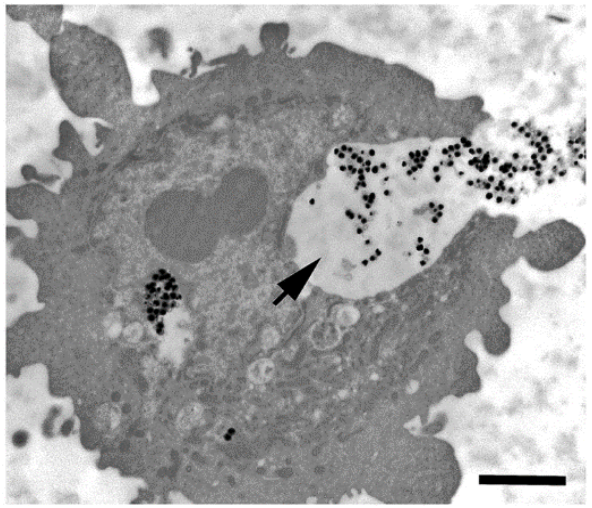

Monteiro-Riviere et al. 2013. Toxicology Letters

- Hill function to simulate endocytosis of gold nanoparticles

$$K_{up,i}(t) = \frac{K_{max,i} \times t^{n_i}}{t_{50,i}^{n_i} + t^{n_i}}$$

$K_{max,i}$: maximum uptake rate

$K_{50,i}$: time reaching half maximum rate

n_i: Hill coefficient

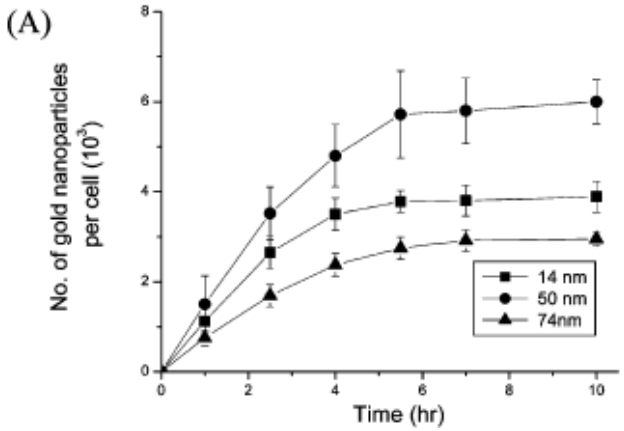

Chithrani et al. 2006. Nano Letters

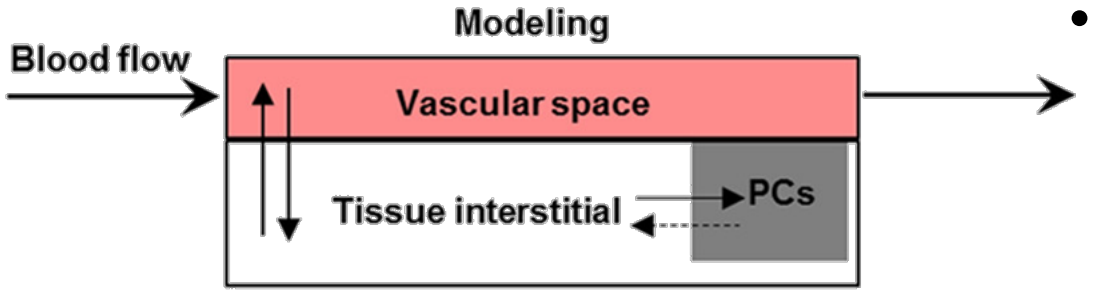

- Simplified equation in PBPK model

$$\frac{dA_{T_i}}{dt} = -K_{up_i} \times A_{T_i} + K_{re,i} \times A_{PC_i}$$

Lin et al., 2016. Nanotoxicology

PCs represent phagocytic cells in organs or tumors;
A_(Ti) represents amount of NPs in the tissue interstitium of the organ;
Kre,i is the release rate constant of NMs by PCs
Physiological based pharmacokinetic (PBPK) model

PBPK model for tumor-bearing mice

Physiological based pharmacokinetic (PBPK) model for tumor-bearing mice

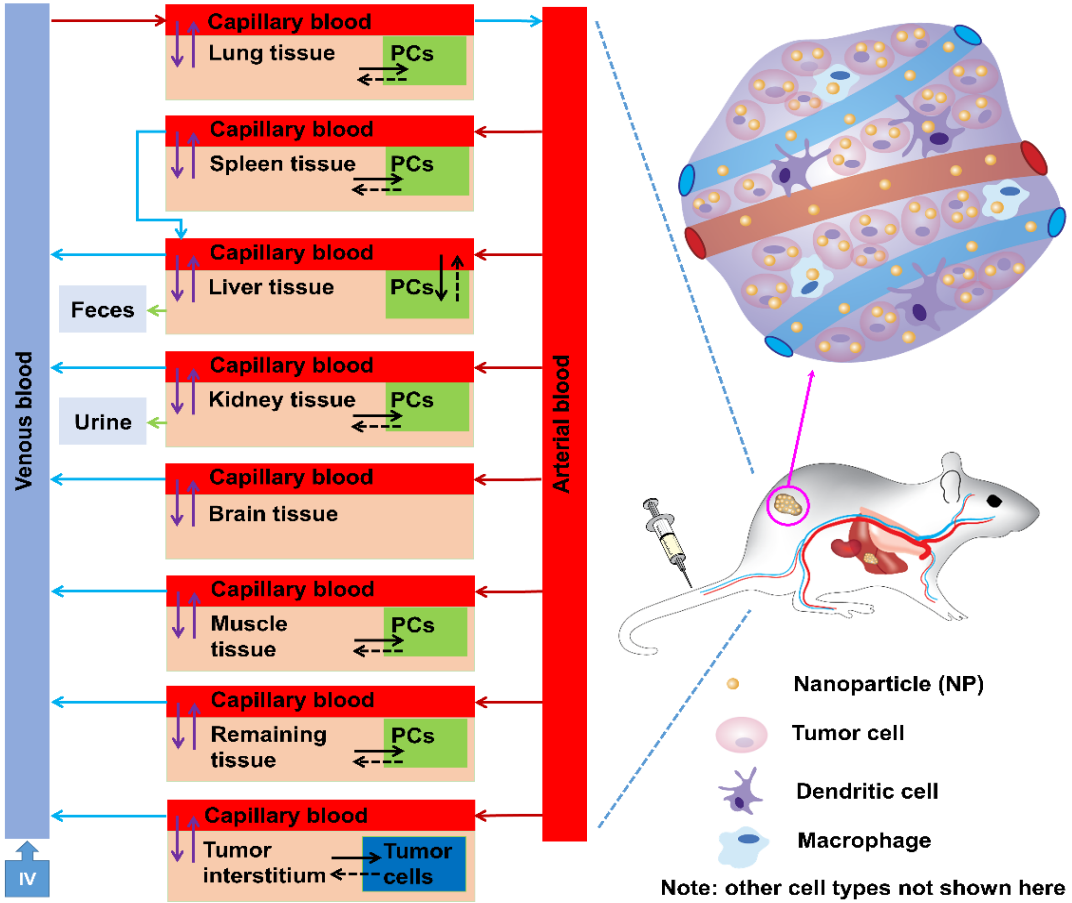

PCs represent phagocytic cells in organs or tumors;

Model fitting with animal studies

Nano Tumor Database: (376 datasets from 200 studies)

CNR or New Ref. ID	New Ref. No	Type	MAT	TS	CT	TM	Shape	log(HD)	ZP	DE(Tmax)	DE(Tmax)_PK	DE(24)	DE(168)	Max DE	log(DE(Tmax))	log(DE(Tmax)_PK)	log(DE(24))	log(DE(168))	log(Max DE)	Conf. in Predict.
#1 Zhong et al. (2015)	1	Inorganic	Gold	Active	Cervix	XH	Rod	1.38	-18	2.06	1.97	1.69	2.06	2.36	0.31	0.29	0.23	0.31	0.37	Y (R2 = 0.99)
#3 Goodrich et al. (2010)	2	Inorganic	Gold	Passive	Colon	AH	Rod	1.48	0	1.62	1.51	0.99	0.79	2.39	0.21	0.18	0	-0.1	0.38	Y (R2 = 0.99)
#4 Meyers et al. (2015)	3	Inorganic	Gold	Passive	Brain	XH	Spherical	1.58	-5	2.99	3.61	6.64	2.99	7.44	0.48	0.56	0.82	0.48	0.87	Y (R2 = 0.87)
#4 Meyers et al. (2015)	3	Inorganic	Gold	Active	Brain	XH	Spherical	1.62	-5	2.83	2.85	3.27	2.83	4.18	0.45	0.45	0.51	0.45	0.62	Y (R2 = 0.87)
#5 Dam et al. (2015)	4	Inorganic	Gold	Active	Breast	XH	Other	1.84	-9.3	0.74	0.64	0.42	1.67	1.77	-0.13	-0.19	-0.38	0.22	0.25	Y (R2 = 0.91)
#6 Sykes et al. (2014)	5	Inorganic	Gold	Active	Skin	XO	Spherical	1.69	-0.6	25.2	25.07	22.86	11	29.88	1.4	1.4	1.36	1.04	1.48	Y (R2 = 0.96)
#6 Sykes et al. (2014)	5	Inorganic	Gold	Active	Skin	XO	Spherical	1.78	-11	25.83	23.86	26.63	9.94	30.24	1.41	1.38	1.43	1	1.48	Y (R2 = 0.96)
#6 Sykes et al. (2014)	5	Inorganic	Gold	Active	Skin	XO	Spherical	2	-9	24.4	21.37	26.87	8.77	29.78	1.39	1.33	1.43	0.94	1.47	Y (R2 = 0.96)
#6 Sykes et al. (2014)	5	Inorganic	Gold	Passive	Skin	XO	Spherical	1.67	-6.7	19.38	18.64	18.11	7.79	23.4	1.29	1.27	1.26	0.89	1.37	Y (R2 = 0.96)
#6 Sykes et al. (2014)	5	Inorganic	Gold	Passive	Skin	XO	Spherical	1.81	-15	14.63	14.28	14.71	5.47	17.52	1.17	1.15	1.17	0.74	1.24	Y (R2 = 0.96)
#6 Sykes et al. (2014)	5	Inorganic	Gold	Passive	Skin	XO	Spherical	2.02	-10	12.17	11.19	11.98	4.53	14.77	1.09	1.05	1.08	0.66	1.17	Y (R2 = 0.96)
#6 Sykes et al. (2014)	5	Inorganic	Gold	Active	Skin	XO	Spherical	2.24	-5	8.79	8.21	9.61	2.98	11.15	0.94	0.91	0.98	0.47	1.05	Y (R2 = 0.96)
#6 Sykes et al. (2014)	5	Inorganic	Gold	Passive	Skin	XO	Spherical	2.22	-6	5.18	4.94	5.63	4.25	6.41	0.71	0.69	0.75	0.63	0.81	Y (R2 = 0.96)
#7 Hu et al. (2014)	6	Inorganic	Gold	Passive	Brain	XH	Spherical	0.79		1.13	1.12	1.13	0.37	1.34	0.05	0.05	0.05	-0.43	0.13	Y (R2 = 0.98)
#8 Razzak et al. (2013)	7	Inorganic	Gold	Passive	Prostate	XH	Spherical	1.44		0.13	0.06	0.11	0.03	0.14	-0.89	-1.22	-0.96	-1.52	-0.85	N (R2 = 0.67)
#9 Liu et al. (2014)	8	Inorganic	Gold	Passive	Cervix	XH	Spherical	1.23	-9.8	1.24	1.13	1.02	0.76	1.55	0.09	0.05	0.01	-0.12	0.19	Y (R2 = 0.94)
#9 Liu et al. (2014)	8	Inorganic	Gold	Passive	Cervix	XH	Spherical	1.49	-10.5	0.64	0.54	0.7	0.32	0.86	-0.19	-0.27	-0.15	-0.49	-0.07	Y (R2 = 0.94)
#10 Cheng et al. (2014)	9	Inorganic	Gold	Active	Brain	XH	Other	1.38	-21.3	1.63	1.57	1.58	0.65	1.87	0.21	0.2	0.2	-0.19	0.27	Y (R2 = 0.97)
#10 Cheng et al. (2014)	9	Inorganic	Gold	Passive	Brain	XH	Other	1.41	21.7	0.61	0.59	0.57	0.26	0.69	-0.21	-0.23	-0.24	-0.59	-0.16	Y (R2 = 0.97)
#10 Cheng et al. (2014)	9	Inorganic	Gold	Passive	Brain	XH	Other	1.32	24.6	0.55	0.51	0.54	0.22	0.61	-0.26	-0.29	-0.27	-0.66	-0.21	Y (R2 = 0.97)
#10 Cheng et al. (2014)	9	Inorganic	Gold	Passive	Brain	XH	Other	1.26	25.4	0.38	0.36	0.4	0.15	0.43	-0.42	-0.44	-0.4	-0.82	-0.37	Y (R2 = 0.97)
#11 Zhang et al. (2015)	10	Inorganic	Gold	Active	Stomach	XH	Spherical	0.79	-5	9.1	9.52	10.68	9.1	12.46	0.96	0.98	1.03	0.96	1.1	Y (R2 = 0.82)
#12 Black et al. (2014)	11	Inorganic	Gold	Passive	Breast	AH	Spherical	1.84	0	4.02	1.74	4.02	2.11	6.09	0.6	0.24	0.6	0.32	0.78	Y (R2 = 0.99)
#12 Black et al. (2014)	11	Inorganic	Gold	Passive	Breast	AH	Other	2.05	0	1.65	0.62	1.65	0.55	2.14	0.22	-0.21	0.22	-0.26	0.33	Y (R2 = 0.99)
#12 Black et al. (2014)	11	Inorganic	Gold	Passive	Breast	AH	Plate	2.12	0	1.23	0.46	1.23	0.37	1.46	0.09	-0.34	0.09	-0.43	0.16	Y (R2 = 0.99)
#12 Black et al. (2014)	11	Inorganic	Gold	Passive	Breast	AH	Rod	1.89	0	0.47	0.15	0.47	0.17	0.61	-0.33	-0.82	-0.33	-0.77	-0.21	Y (R2 = 0.99)
#13 Liu et al. (2013)	12	Inorganic	Gold	Passive	Breast	XO	Spherical	0.74	0	1.26	1.24	1.54	0.41	1.74	0.1	0.09	0.19	-0.39	0.24	Y (R2 = 0.70)
#14 Karmani et al. (2013)	13	Inorganic	Gold	Active	Skin	XO	Spherical	1.49		2.25	2.23	1.53	2.25	2.52	0.35	0.35	0.18	0.35	0.4	Y (R2 = 0.97)
#15 Wang et al. (2012)	14	Inorganic	Gold	Passive	Breast	AH	Other	1.8	10.2	2.67	2.45	2.67	0.8	3.07	0.43	0.39	0.43	-0.1	0.49	Y (R2 = 0.99)
#15 Wang et al. (2012)	14	Inorganic	Gold	Passive	Breast	AH	Other	1.98	18.7	0.48	0.44	0.48	0.14	0.52	-0.32	-0.36	-0.32	-0.85	-0.28	Y (R2 = 0.99)
#16 Shah et al. (2012)	15	Inorganic	Gold	Passive	Prostate	XH	Spherical	1.82	-2.6	0.67	0.64	0.67	0.21	0.79	-0.17	-0.19	-0.17	-0.68	-0.1	Y (R2 = 0.99)
#16 Shah et al. (2012)	15	Inorganic	Gold	Passive	Prostate	XH	Spherical	1.8	-27.1	0.6	0.59	0.6	0.17	0.71	-0.22	-0.23	-0.22	-0.77	-0.15	Y (R2 = 0.99)
#16 Shah et al. (2012)	15	Inorganic	Gold	Active	Prostate	XH	Spherical	1.86	-2.9	0.61	0.55	0.61	0.21	0.85	-0.21	-0.26	-0.21	-0.68	-0.07	Y (R2 = 0.99)

Obtain optimized model parameters

Finalized PBPK model

Chou WC, Chen Q, Yuan L, Cheng YH, He C, Monteiro-Riviere NA, Riviere JE, Lin Z. An artificial intelligence-assisted physiologically-based pharmacokinetic model to predict nanoparticle delivery to tumors in mice. J Control Release. 2023 Sep;361:53-63

Similarity between predicted and data-driven parameters

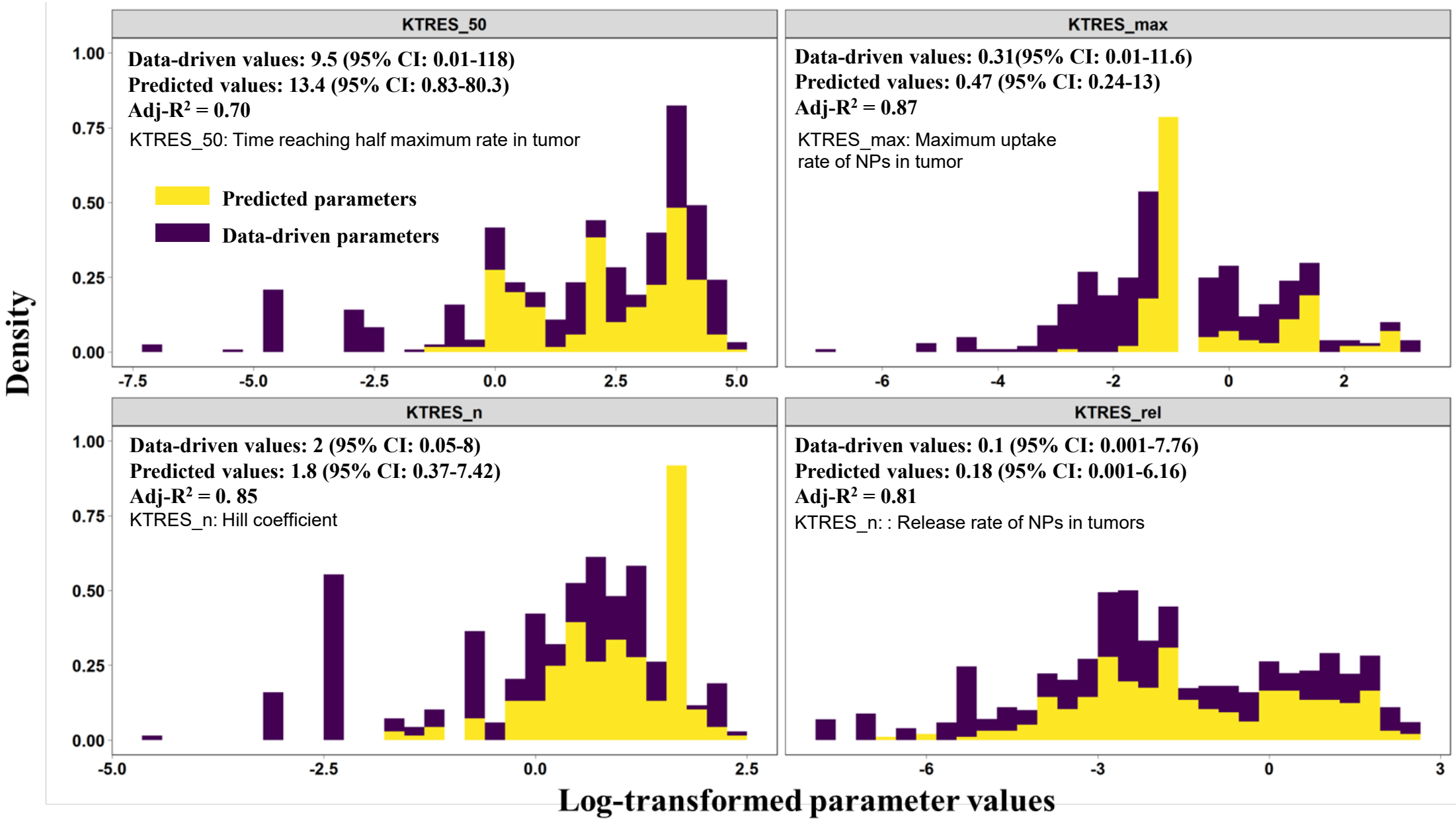

Evaluation results of AI-PBPK model-predicted tumor delivery efficiency

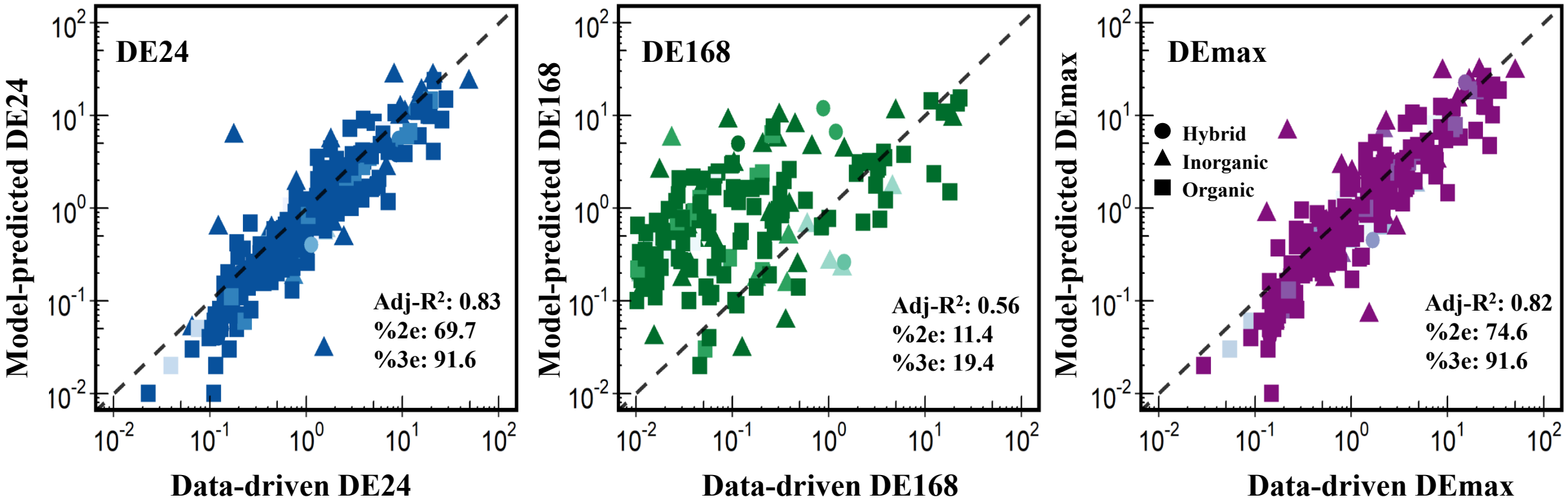

Abbreviation: DE, delivery efficiency; DE24, delivery efficiency at 24 hours; DE168, delivery efficiency at 168 hours; Demax, maximum of DE; %2e, percentage of 2-fold error range %3e, percentage of 3-fold error range

Evaluation results of AI-PBPK model-predicted time-dependent distribution of nanoparticles (NPs) to tumors

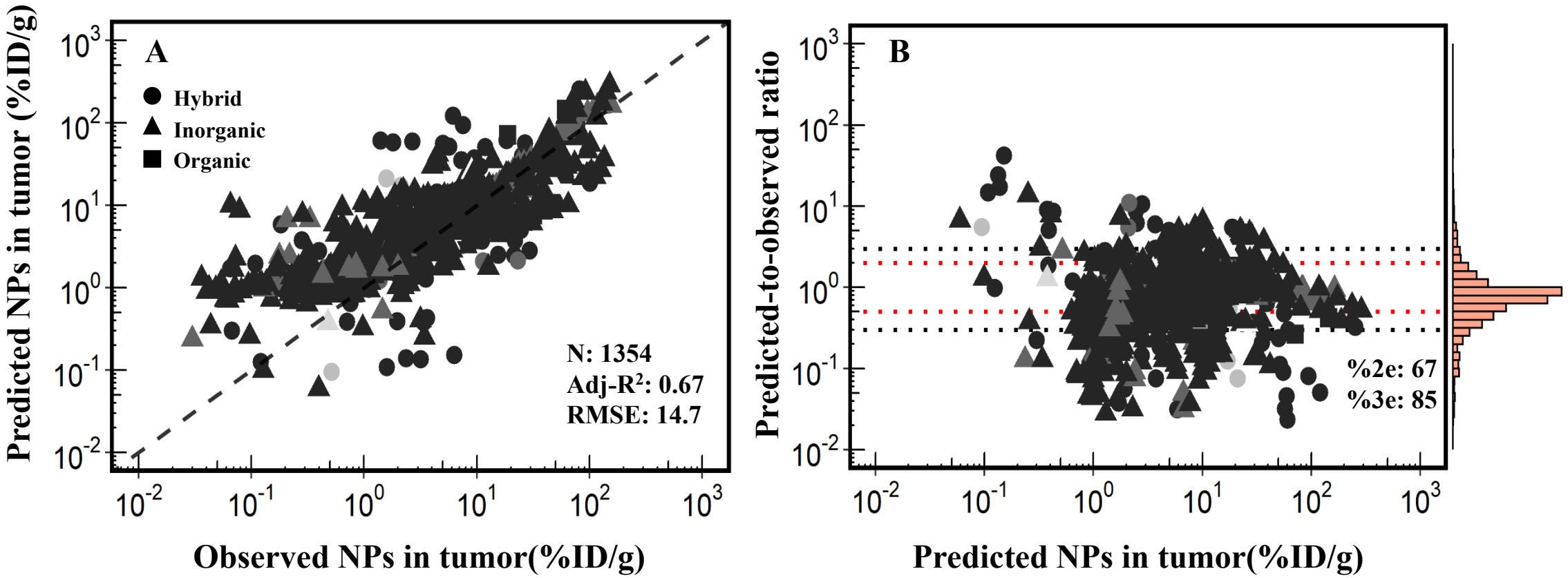

Representative evaluation results of AI-PBPK model

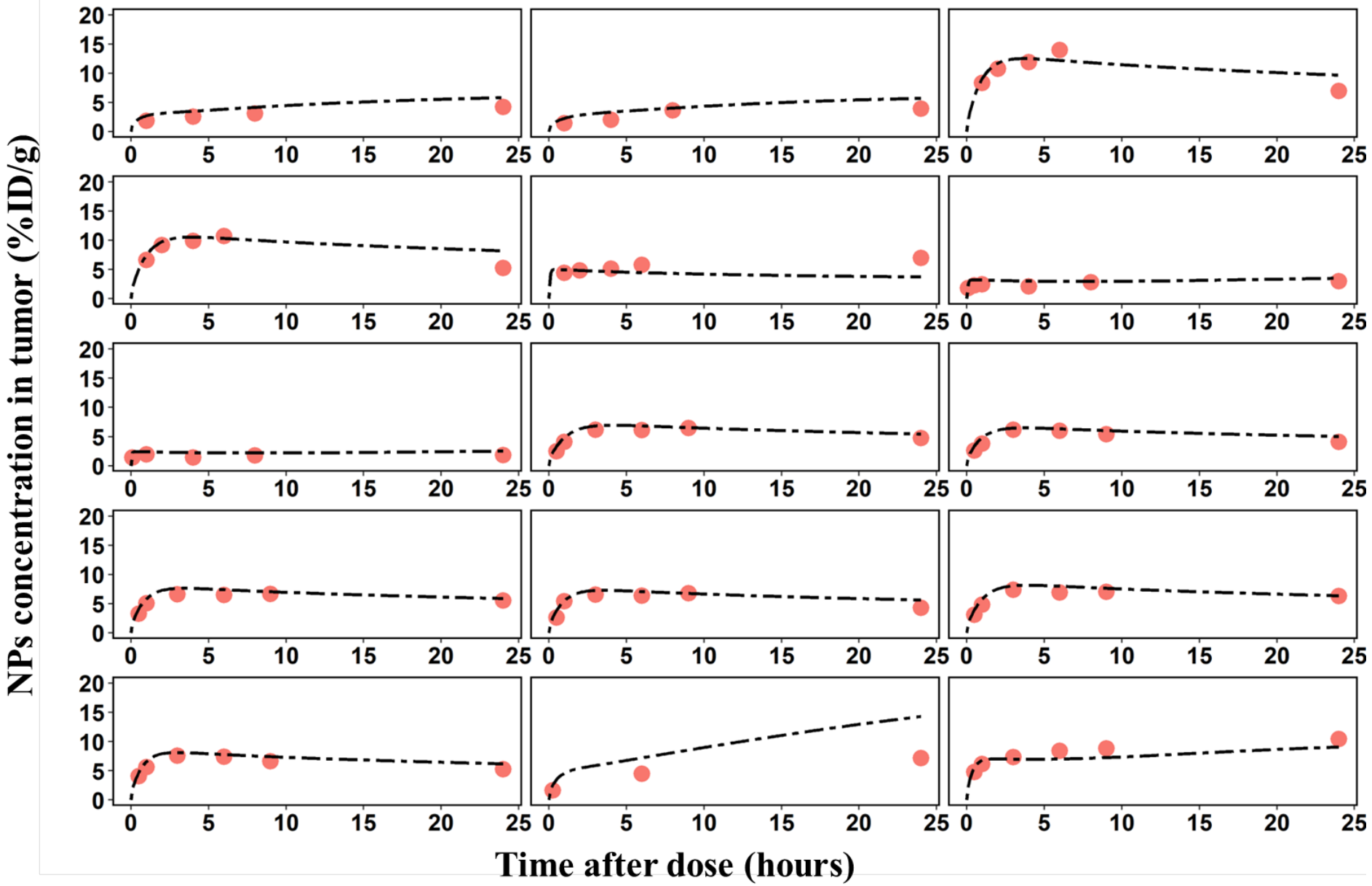

Summary for hybrid method

- This study demonstrated the feasibility of an integration of machine learning/AI technologies with a mechanistic PBPK model to predict the tumor delivery efficiency of NPs.

- Our AI-assisted PBPK model not only provides an early screening tool for estimating tumor delivery efficiency of NPs, but also can reduce the number of animals use at the early-stage preclinical trials to identify NPs with desired delivery efficiency to tumor.

Acknowledgements

Lab members:

Zhoumeng Lin
Wei-Chun Chou
Qiran Chen
Malek Hussein Hajjawi
Xue Wu
Pei-Yu Wu
Chi-Yu Chen
Zhicheng Zhang
Venkata Nithin Kamineni
Yashas Kuchimanchi

Former members:

Miao Li
Yi-Hsien Cheng
Md Mahbubul Huq Riad
Long Yuan
Dongping Zeng
Trevor Elwell-Cuddy
Paula Solar; Sichao Mao
Yilei Zheng; Yi-Jun Lin
Ning Xu; Yu Shin Wang
Jake Willson
Gabriel (Guanyu) Tao

Collaborators:

ICCM/NICKS/KSU
EGH/CEHT/UF
FARAD Team

Advisors:

Dr. Jim E. Riviere
Dr. Nancy A. Monteiro-Riviere
Dr. Nikolay M. Filipov
Dr. Jeffrey W. Fisher
Dr. Ronette Gehring

Funding:

- NIH/NIBIB Grant #: R01EB031022
- NIH/NIBIB Grant #: R03EB026045
- NIH/NIBIB Grant #: R03EB025566
- UF PHHP PhD Fellowship in Artificial Intelligence

KSU Lab 2019

UF Lab 2021

National FARAD 2022

UF Lab 2023

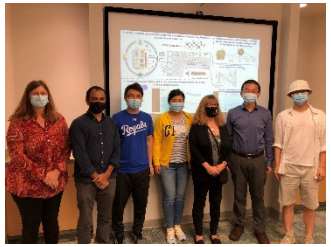

UF FARAD 2021

National FARAD 2022